

# Titan Cells Confer Protection from Phagocytosis in *Cryptococcus neoformans* Infections

Laura H. Okagaki and Kirsten Nielsen

Department of Microbiology, Medical School, University of Minnesota, Minneapolis, Minnesota, USA

**The human fungal pathogen *Cryptococcus neoformans* produces an enlarged “titan” cell morphology when exposed to the host pulmonary environment. Titan cells exhibit traits that promote survival in the host. Previous studies showed that titan cells are not phagocytosed and that increased titan cell production in the lungs results in reduced phagocytosis of cryptococcal cells by host immune cells. Here, the effect of titan cell production on host-pathogen interactions during early stages of pulmonary cryptococcosis was explored. The relationship between titan cell production and phagocytosis was found to be nonlinear; moderate increases in titan cell production resulted in profound decreases in phagocytosis, with significant differences occurring within the first 24 h of the infection. Not only were titan cells themselves protected from phagocytosis, but titan cell formation also conferred protection from phagocytosis to normal-size cryptococcal cells. Large particles introduced into the lungs were not phagocytosed, suggesting the large size of titan cells protects against phagocytosis. The presence of large particles was unable to protect smaller particles from phagocytosis, revealing that titan cell size alone is not sufficient to provide the observed cross-protection of normal-size cryptococcal cells. These data suggest that titan cells play a critical role in establishment of the pulmonary infection by promoting the survival of the entire population of cryptococcal cells.**

*Cryptococcus neoformans* is a human fungal pathogen that primarily infects immunocompromised patient populations (6). The recent rise in the number of HIV-positive (HIV<sup>+</sup>) patients, patients receiving chemotherapy, and organ transplant recipients has resulted in an increase in the incidence of cryptococcal infections (6). Cryptococcal infections are now the third leading cause of death in sub-Saharan Africa and are responsible for more deaths than *Mycobacterium tuberculosis* (18). Cryptococcosis can manifest as skin lesions, pulmonary infection, and meningitis—the deadliest stage of the disease (6). In a typical infection, cryptococcal spores or desiccated yeast cells are inhaled into the lungs. These small particles lodge in the alveoli, where they can establish a pulmonary infection. At later stages of infection, cryptococcal cells can escape from the lungs and disseminate throughout the body, eventually penetrating the blood-brain barrier to cause meningitis. In sub-Saharan Africa, approximately 60% of HIV<sup>+</sup> patients succumb to cryptococcal infections (6, 18).

Upon exposure to the host pulmonary environment, a subset of cryptococcal cells found in the lungs undergo a morphological change, producing enlarged “titan” cells. Approximately 20% of cells in the lungs become titan cells, while the remaining cells are equivalent in size to cryptococcal cells grown *in vitro* (15). Cryptococcal cells grown *in vitro* are typically 5 to 10  $\mu\text{m}$  in diameter, but titan cells can be as large as 50 to 100  $\mu\text{m}$  in diameter (15, 25). Titan cell production in *Cryptococcus* has been observed as early as 24 h postinfection and is primarily observed in the lungs, suggesting a role for titan cells in the early pulmonary infection (15). Titan cell production in response to the host pulmonary environment is regulated via the protein kinase A (PKA) pathway (16, 25), which regulates the production of other cryptococcal virulence factors, including the thick antiphagocytic polysaccharide capsule and the dark pigment melanin that protects cryptococcal cells from nitrosative and oxidative stress (3).

Titan cells exhibit several characteristics that suggest they have altered host-pathogen interactions. Under host temperature and nutrient conditions, *C. neoformans* produces a thick polysaccha-

ride capsule (6). The capsule is able to bind both antibody and complement C3, reducing phagocytosis by host macrophages (6). In *Cryptococcus*, the capsule of a normal-size cell recovered from the lungs appears fibrous under electron microscopy and is shed easily into the host environment (25). However, the capsule of titan cells is highly cross-linked and is unable to be sheared from the cells by chemical or physical means (25). Titan cells also exhibit a thickened cell wall that appears to be 20- to 30-fold thicker than the cell wall of normal-size cells (25). In addition, titan cells are more resistant to the antimicrobial oxidative and nitrosative stresses produced by the host immune response (15, 25).

Previous studies showed that increased titan cell production also results in lowered phagocytosis (15, 25); however, the nature of the reduction in phagocytosis remained unknown. Here, the role of titan cell production in protection from phagocytosis was further examined. We show that titan cells can confer protection to normal-size cells during early stages of pulmonary infection. While the large size of titan cells can provide protection from phagocytosis, size alone is not sufficient to provide cross-protection to smaller cells. These data show that the role for titan cell production during early pulmonary cryptococcosis extends beyond simple protection of the titan cell due to its large size and suggest that titan cell production alters global interactions between *C. neoformans* and the host.

## MATERIALS AND METHODS

**Ethics statement.** All animals were handled in strict accordance with good animal practice, as defined by the relevant national and/or local animal

Received 17 April 2012 Accepted 18 April 2012

Published ahead of print 27 April 2012

Address correspondence to Kirsten Nielsen, knielsen@umn.edu.

Copyright © 2012, American Society for Microbiology. All Rights Reserved.

doi:10.1128/EC.00121-12

welfare bodies. All animal work was approved by the University of Minnesota Institutional Animal Care and Use Committee (IACUC) under protocol no. 0712A22250 and 1010A91133.

**Strains and media.** The *C. neoformans* var. *grubii* strains KN99 $\alpha$  (wild type) (11), MutX 31-1 (*otc1* $\Delta$ ) (Okagaki and Nielsen, unpublished observation), YPH308 (*otc1* $\Delta$  *gpa2* $\Delta$  *gpa3* $\Delta$ ) (7), CDX18 (*gpr4* $\Delta$  *gpr5* $\Delta$ ) (16, 24), and CDX11 (*gpr5* $\Delta$ ) (16) were used in this study. Strains were stored as glycerol stocks at  $-80^{\circ}\text{C}$  and grown at  $30^{\circ}\text{C}$  in yeast extract-peptone-dextrose (YPD) agar or broth medium (BD, Hercules, CA).

**In vivo titan cell and phagocytosis assay.** *C. neoformans* cells were cultured overnight in YPD broth. The resulting yeast cells were pelleted and resuspended in sterile phosphate-buffered saline (PBS) at a concentration of  $1 \times 10^8$  cells/ml based on hemocytometer count. Groups of 6- to 8-week-old female C57BL/6 mice (Jackson Laboratory, Bar Harbor, ME) were anesthetized by intraperitoneal pentobarbital injection. Three to five mice per treatment were infected intranasally with  $5 \times 10^6$  cells in 50  $\mu\text{l}$  PBS (Lonza, Rockland, ME). Mice were sacrificed by  $\text{CO}_2$  inhalation at 24, 48, or 72 h postinfection. Lungs were lavaged with 1.5 ml sterile PBS three times using an 18.5-gauge needle placed in the trachea. Cells in the lavage fluid were pelleted at  $16,000 \times g$ , resuspended in 3.7% formaldehyde, and incubated at room temperature for 30 min. Cells were then washed once with PBS, and  $>500$  cells per animal were analyzed for size and phagocytosis by microscopy (AxioImager, Carl Zeiss, Inc.). Cell body size was measured, and cells were classified as small cells ( $<10 \mu\text{m}$  in diameter) or titan cells ( $>10 \mu\text{m}$  in diameter).

**Coinfections.** KN99 $\alpha$  and the *gpr5* $\Delta$  strain were fluorescently labeled with Alexa Fluor 488 (AF488) or Alexa Fluor 594 (AF594) (Invitrogen, Grand Island, NY) as described previously (15). Three to five mice per treatment were infected as described above with  $5 \times 10^6$  AF488-labeled KN99 $\alpha$ , AF594-labeled *gpr5* $\Delta$  mating type  $\alpha$ , or an approximate 1:1 ratio of fluorescently labeled KN99 $\alpha$  and the *gpr5* $\Delta$  strain. Infected mice were sacrificed at 3 days postinfection by  $\text{CO}_2$  inhalation. Samples were collected by lavage and fixed as described above. Greater than 500 cells per animal were analyzed for size, phagocytosis, and fluorescence by microscopy (AxioImager, Carl Zeiss, Inc.).

**In vivo bead phagocytosis assay.** Inert polystyrene beads (Phosphorex, Inc., Fall River, MA) were opsonized based on the protocol by Cannon et al. (1). Briefly, 10- $\mu\text{m}$  or 30- $\mu\text{m}$  beads were washed with sterile PBS and then incubated with 10 mg/ml bovine serum albumin (Sigma-Aldrich, St. Louis, MO) in PBS at  $4^{\circ}\text{C}$  for 2 h. Following incubation, the beads were washed with PBS, resuspended in 0.5 mg/ml of rabbit polyclonal anti-bovine serum albumin (anti-BSA) IgG (AbCam, Cambridge, MA) in PBS for 30 min at  $37^{\circ}\text{C}$ , followed by incubation at  $4^{\circ}\text{C}$  for 10 min. Beads were then washed with PBS and stained with Alexa Fluor 350 (30  $\mu\text{m}$ ) or Alexa Fluor 594 (10  $\mu\text{m}$ ) as described above. Three to five 6- to 8-week-old C57BL/6 mice (Jackson Laboratory, Bar Harbor, ME) were intranasally infected as described above with  $3.5 \times 10^6$  beads in 50  $\mu\text{l}$  PBS. At 3 days postinoculation, lungs were lavaged with 1.5 ml PBS three times as described above. Beads and cells in the lavage fluid were pelleted at  $16,000 \times g$ , resuspended in 3.7% formaldehyde, and incubated at room temperature for 30 min. Samples were then washed once with PBS and resuspended in PBS. Greater than 100 beads per animal were analyzed for size, phagocytosis, and fluorescence by microscopy (AxioImager; Carl Zeiss, Inc.).

**Effect of cell age on in vivo phagocytosis.** Three to five mice per treatment were infected as described above with  $5 \times 10^6$  cells of the AF488-labeled strain KN99 $\alpha$ , the AF488-labeled *otc1* $\Delta$  strain, the AF594-labeled *gpr5* $\Delta$  strain, or the AF594-labeled *gpr4* $\Delta$  *gpr5* $\Delta$  mating type  $\alpha$  strain. Infected mice were sacrificed at 3 days postinfection by  $\text{CO}_2$  inhalation. Lungs were lavaged with 1.5 ml sterile PBS three times using an 18.5-gauge needle placed in the trachea. Cells in the lavage fluid were pelleted at  $16,000 \times g$ , resuspended in 3.7% formaldehyde, and incubated at room temperature for 30 min. Cells were then washed once with PBS and resuspended in PBS. Greater than 2,000 cells per animal were ana-

lyzed for size, phagocytosis, and fluorescence by microscopy (AxioImager; Carl Zeiss, Inc.).

**Statistical analysis.** All analyses were performed using Analyze-It (Analyze-It, Ltd., Leeds, England). One-way analysis of variance (ANOVA) was used to analyze differences in titan cell production and phagocytosis. *P* values of  $<0.05$  were considered significant. For coinfections, Wilcoxon's rank sum test was used to analyze differences in the hypothesized percentage of phagocytosis, based on half of the phagocytosis observed in individual infections and the observed percentage of phagocytosis during coinfection. *P* values of  $<0.05$  were considered significant.

## RESULTS

**Size alone can protect against phagocytosis.** *Cryptococcus* is typically inhaled into the lungs and lodges in alveoli. At early stages of infection, the primary innate immune cells present in the lungs are resident alveolar macrophages (6). Thus, early interactions between *Cryptococcus* and alveolar macrophages are critical for the survival of fungal cells and establishment of infection. We showed previously that titan cells are not phagocytosed in the lungs (15). While titan cells can be 50 to 100  $\mu\text{m}$  in diameter (15, 25), alveolar macrophages are generally only 10 to 20  $\mu\text{m}$  in diameter (1). These data suggest that titan cells could be protected from phagocytosis due to their large size.

To determine if titan cells could be protected from phagocytosis based on their size alone, large and small inert polystyrene beads were introduced into the lungs of mice by the intranasal infection model typically used for titan cell experiments. Thirty-micrometer beads were used to simulate the large titan cells, while 10- $\mu\text{m}$  beads were used to simulate normal-size cryptococcal cells. The beads were opsonized with BSA followed by anti-BSA IgG to simulate recognition of the titan or normal-size cryptococcal cells and to stimulate the interaction with phagocytes and subsequent phagocytosis. At 3 days postinoculation, beads were recovered by bronchoalveolar lavage (BAL). Samples were fixed immediately and examined for phagocytosis by microscopy. Approximately 90% of the 10- $\mu\text{m}$  beads were phagocytosed, showing that normal-size cryptococcal cells are small enough to be phagocytosed by resident alveolar macrophages (Fig. 1A). In contrast, no 30- $\mu\text{m}$  beads were phagocytosed, suggesting that the large size of titan cells could provide protection from phagocytosis (Fig. 1A). These data show that size alone can block phagocytosis and suggest that titan cells could be protected from phagocytosis by their large size.

**Association between phagocytosis and titan cell production is nonlinear.** While titan cells themselves are not phagocytosed (15, 25), the nature of the relationship between titan cell production and cryptococcal cell phagocytosis in the lungs remained unclear. There are at least two possible hypotheses for how titan cell production can reduce phagocytosis (Fig. 2A). First, the titan cells themselves could be protected by size alone, resulting in a direct correlation between titan cell production and phagocytosis—a linear relationship (Fig. 2A, dotted line). Alternatively, titan cell production could result in a global decrease in phagocytosis in which small changes in titan cell production would reduce overall levels of phagocytosis—a nonlinear relationship (Fig. 2A, solid line).

Four strains with differences in titan cell production were utilized to determine the relationship between titan cell formation and phagocytosis: (i) the wild-type strain KN99 $\alpha$ , which exhibited approximately 20% titan cell formation (11); (ii) a *gpr5* $\Delta$  mutant

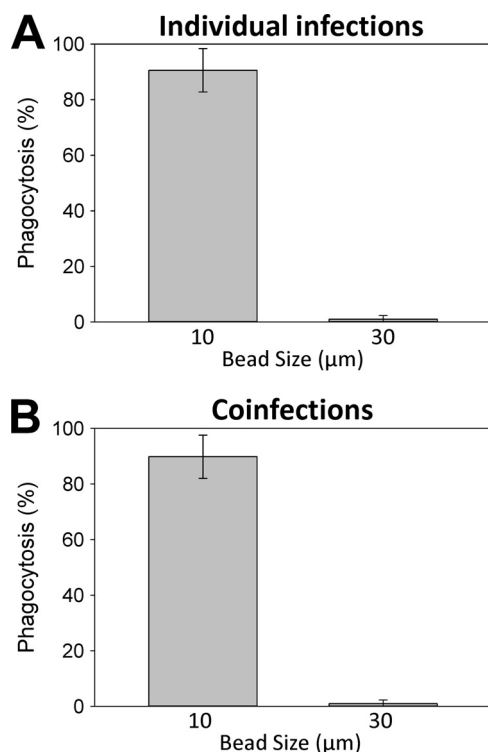


**FIG 1** Large size cannot provide cross-protection from phagocytosis. Mice were intranasally infected with  $3.5 \times 10^6$  large 30-μm or small 10-μm inert beads. At 3 days postinoculation, lungs were lavaged and samples were fixed and examined by microscopy to determine phagocytosis of the beads. (A) Individual infections with either 30-μm inert beads or 10-μm inert beads. (B) Coinfections with a 1:1 ratio of 30-μm and 10-μm beads. Greater than 100 beads were counted per sample. Error bars represent standard deviations for 3 mice per treatment.

strain that produced 2 to 3% titan cells (16); (iii) a *gpr4Δ gpr5Δ* double mutant strain that had minimal titan cell production (16, 24); and (iv) an *otc1Δ* (overproducer of titan cells) mutant strain that produced >50% titan cells by 3 days postinfection. The *otc1Δ* strain contains a mutation in a single gene with unknown function that enhances titan cell production *in vivo* (L. H. Okagaki and K. Nielsen, unpublished observation). All four of these strains demonstrate wild-type levels of other known virulence factors, including growth at 37°C, melanin production, capsule formation, and urease production. Additionally, all four of these strains produce normal-size cells when grown *in vitro*.

Titan cell production and phagocytosis were determined in mice intranasally inoculated with  $5 \times 10^6$  cryptococcal cells. Cells were collected at 3 days postinfection by bronchoalveolar lavage (BAL), fixed immediately, and examined by microscopy for cryptococcal cell size and phagocytosis. The relationship between titan cell production and phagocytosis for all strains was determined (Fig. 2B). The *gpr4Δ gpr5Δ* strain, with no titan cell production, exhibited the highest rate of phagocytosis at approximately 17 to 19% (Fig. 2B, black triangles). The *gpr5Δ* strain, with low levels of titan cell production had slightly less phagocytosis (Fig. 2B, gray diamonds). In contrast, the wild-type (Fig. 2B, white squares) and *otc1Δ* (Fig. 2B, black circles) strains exhibited the lowest levels of phagocytosis, ranging from 0.5 to 2.5% phagocytosis. Linear regression and decay curves were calculated, and  $r^2$  values were de-

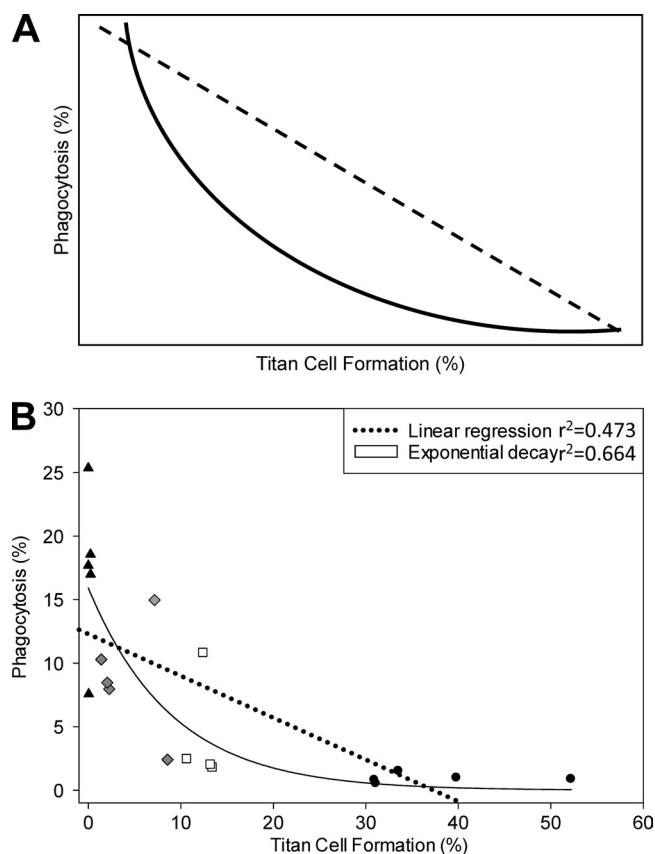


**FIG 2** The relationship between titan cell production and phagocytosis is nonlinear. (A) Two hypothesized relationships between titan cell production and phagocytosis include (i) a linear relationship in which titan cells are protected from phagocytosis by size alone (dotted line) and (ii) a nonlinear relationship in which small amounts of titan cell production result in a global decrease in phagocytosis (solid line). (B) Mice were intranasally inoculated with  $5 \times 10^6$  cells of the wild-type or mutant cryptococcal strains that exhibit altered titan cell formation. At 3 days postinfection, lungs were lavaged, and the resulting BAL samples were fixed and examined by microscopy for titan cell production and phagocytosis. Black triangles, gray diamonds, white squares, and black circles indicate infections with the *gpr4Δ gpr5Δ*, *gpr5Δ*, wild-type, and *otc1Δ* strains, respectively.  $r^2$  values were calculated based on linear regression and exponential decay curves. Four to five mice were inoculated per treatment, and >2,000 cells were examined per mouse.

termined for the data set. The  $r^2$  value for the decay curve ( $r^2 = 0.664$ ) was higher than the linear regression line ( $r^2 = 0.473$ ), and thus the relationship between titan cell formation and phagocytosis fits the decay curve model better than the linear model. These data show that small changes in titan cell production dramatically reduce phagocytosis and suggest that titan cell production has a global effect on phagocytosis.

To determine the time frame in which titan cell production reduced phagocytosis, titan cell production and phagocytosis were monitored at 24, 48, and 72 h postinfection with the *gpr4Δ gpr5Δ*, wild-type, and *otc1Δ* strains (Fig. 3). As observed previously, the *gpr4Δ gpr5Δ* strain had minimal titan cell production over the course of the experiment (Fig. 3A). In contrast, the wild-type strain showed moderate increases in titan cell formation, while the *otc1Δ* mutant strain exhibited significant increases in titan cell production over the course of the experiment (Fig. 3A). Even though the *otc1Δ* strain exhibited differences in titan cell

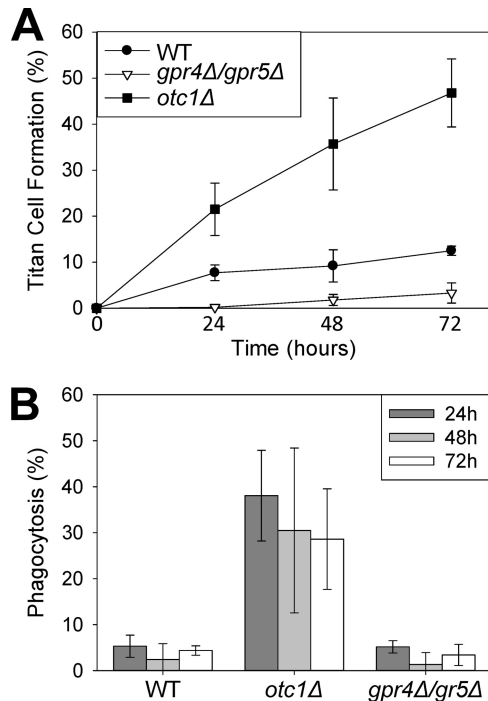


**FIG 3** Titan cell production reduces phagocytosis by 24 h postinfection. Mice were intranasally inoculated with  $5 \times 10^6$  cells of the wild-type (WT), *gpr4Δ* *gpr5Δ*, or *otc1Δ* strains. At 24, 48, or 72 h postinfection, lungs were lavaged, and the resulting samples were fixed immediately. Samples were examined for titan cell production (A) and phagocytosis (B). Error bars represent standard deviations from three to five mice per strain. Greater than 300 cells per mouse were examined.

production over time, no difference in phagocytosis between the time points was observed (Fig. 3B;  $P = 0.27$ ). In fact, no difference in phagocytosis in any of the strains was observed over the course of the experiment ( $P = 0.054$  for the *gpr4Δ gpr5Δ* strain, and  $P = 0.081$  for the wild type), suggesting that titan cell production within the first 24 h of the infection was able to block phagocytosis (Fig. 3B). Consistent with the nonlinear relationship between titan cell production and phagocytosis observed above, the *gpr4Δ gpr5Δ* strain that lacks titan cell formation had significantly more phagocytosis than the strains that generated titan cells ( $P < 0.0001$  for comparisons of individual time points in the *gpr4Δ gpr5Δ* strain and wild-type or *otc1Δ* strain), while no difference in phagocytosis was observed between the wild-type strain that has moderate titan cell formation and the *otc1Δ* strain with high titan cell production ( $P > 0.400$  for comparisons of individual time points in the wild-type and *otc1Δ* strains).

These data show that as little as 10% titan cell production almost completely abolished phagocytosis of all cryptococcal cells during the early pulmonary infection. Thus, titan cell production resulted in a global decrease in phagocytosis that did not directly correlate with the number of titan cells present in the sample. Not only were titan cells themselves protected from phagocytosis, but the presence of titan cells reduced overall levels of phagocytosis.

**Nascent cells exhibit reduced titan cell formation and phagocytosis.** The time course data presented above show that titan cell production during the first 24 h of the infection dramatically decreased phagocytosis, but additional titan cell formation at later times did not provide any further benefit. Previous studies exam-

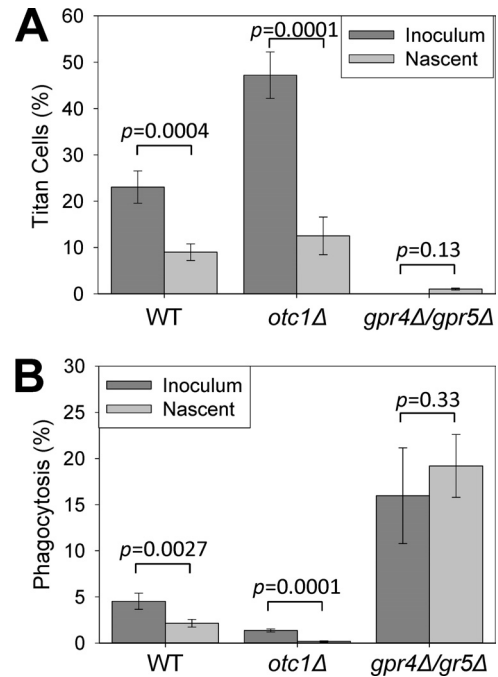


**FIG 4** Nascent cells exhibit reduced phagocytosis. Mice were intranasally infected with  $5 \times 10^6$  cells of Alexa Fluor 488-labeled wild-type (WT) cells, Alexa Fluor 488-labeled *otc1Δ* cells, or Alexa Fluor 594-labeled *gpr5Δ* cells. At 3 days postinfection, lungs were lavaged and the samples were fixed and examined by microscopy. Titan cell formation (A) and phagocytosis (B) were quantified in unstained and stained populations of cells in each lavage sample. Error bars indicate standard deviations from three to five mice per strain and  $>2,000$  cells per mouse.

ining transcriptional changes in response to phagocytosis by macrophages *in vitro* suggest that cryptococcal cells inhaled into the lungs need time to adjust to the host environment (4). Thus, the initial infecting inoculums may exhibit higher rates of phagocytosis and benefit more from titan cell production, whereas cells that have already adapted to the host environment may not benefit from titan cell production.

To test this hypothesis, mice were infected with cryptococcal cells stained with AF488 or AF594. These stains bind to components in the cryptococcal cell wall that are not transferred to the daughter cell upon cell division. Thus, only the initial inoculum was fluorescently labeled, while nascent daughter cells produced *in vivo* were unlabeled. Mice were infected with the fluorescently labeled wild-type, *otc1Δ*, or *gpr4Δ gpr5Δ* strains. At 72 h postinfection, cells were recovered from the lungs by BAL and fixed, and phagocytosis, titan cell production, and fluorescence were determined by microscopy.

Titan cell production by cells in the original inoculum was higher than that observed for the *in vivo*-produced nascent cells for both the wild-type and *otc1Δ* strains (Fig. 4A). In the wild-type strain, cells in the original inoculum produced approximately 20% titan cells, while the nascent cells exhibited only 10% titan cell production (Fig. 4A;  $P = 0.0004$ ). A similar trend was observed in the *otc1Δ* mutant, where titan cell production in the nascent cells was one-fifth that observed in the original inoculum (Fig. 4A;  $P = 0.0001$ ). Interestingly, infections with the wild-type strain exhibited phagocytosis rates of approximately 5% in the original inoculum, and phagocytosis was significantly reduced in



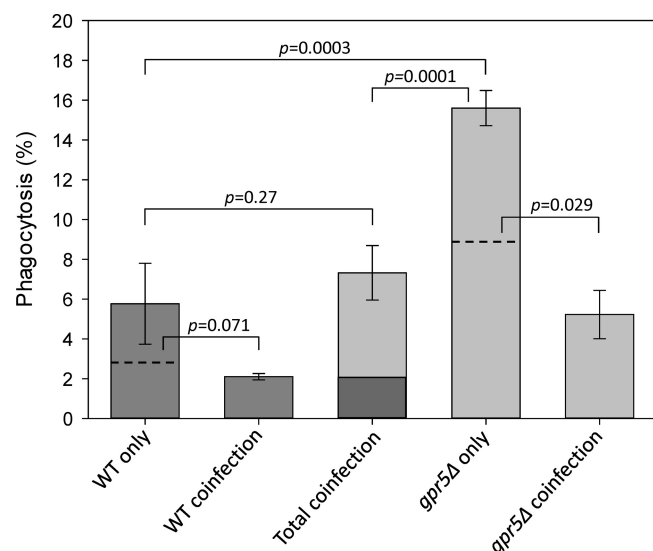


**FIG 5** Titan cell production provides cross-protection from phagocytosis to normal-size cryptococcal cells. Mice were intranasally inoculated with  $5 \times 10^6$  cells of Alexa Fluor 488-stained wild-type (WT) cells, Alexa Fluor 594-stained *gpr5Δ* cells, or an approximate 1:1 ratio of wild-type and *gpr5Δ* cells. At 3 days postinfection, lungs were lavaged, and the BAL samples were fixed and examined by microscopy for titan cell production, phagocytosis, and fluorescence. Dotted lines indicate half of the phagocytosis observed in the individual infections. The “total coinfection” bar indicates the total amount of phagocytosis observed during the coinfection with wild-type cells indicated in dark gray and *gpr5Δ* cells indicated in light gray. Error bars represent standard deviations from three to five mice per treatment with  $>500$  cells examined per mouse.

the nascent cells produced *in vivo* to 2.5% (Fig. 4B;  $P = 0.0027$ ). Similar results were observed with the titan cell-overproducing *otc1Δ* strain in which phagocytosis of the nascent cells was almost completely abolished (Fig. 4B;  $P = 0.0001$ ). Neither titan cell production nor phagocytosis was altered in the *gpr4Δ gpr5Δ* nascent cells compared to cells in the original inoculum (Fig. 4;  $P = 0.13$  and  $P = 0.33$ , respectively), suggesting that early production of titan cells was required to alter phagocytosis of the nascent cells produced *in vivo* and any subsequent titan cell formation by the newly formed cryptococcal cells. These data suggest that titan cells produced in the first 24 h of the infection influence both protection from phagocytosis and titan cell formation in the subsequent nascent cell populations.

**Titan cell production protects normal-size cryptococcal cells from phagocytosis.** Titan cells produced in the first 24 h of the infection reduced phagocytosis of nascent cells produced *in vivo*. In addition, titan cell production resulted in a global decrease in phagocytosis in a nonlinear manner. These data suggested titan cell production may protect normal-size cryptococcal cells from phagocytosis.

To test this hypothesis directly, we coinfectd the *gpr5Δ* strain that has limited titan cell production with the wild-type strain that has approximately 20% titan cell production (Fig. 5). The goal of this experiment was to see if the titan cells generated by the wild-type strain could protect the *gpr5Δ* cells from phagocytosis. Mice were intranasally inoculated with  $5 \times 10^6$  AF488-labeled wild-type cells, AF594-labeled *gpr5Δ* cells, or a 1:1 ratio of fluorescently labeled wild-type and *gpr5Δ* cells. At 3 days postinfection, cells were recovered from the lungs by BAL, fixed, and examined for phagocytosis. In the coinfection, wild-type cells were identified by

their green fluorescence (AF488), while *gpr5Δ* cells were identified by their red fluorescence (AF594). The total numbers of cells in the inoculums ( $5 \times 10^6$  cells) were the same for the individual infections and the coinfections. Because the coinfections contained equal ratios of the two strains, half the number of cells of each strain was present in the coinfections compared to the numbers in the individual infections.

If titan cell production did not confer protection from phagocytosis to normal-size cryptococcal cells, then the coinfections would exhibit half the amount of phagocytosis for each strain compared to that observed during individual infections (indicated by dotted lines in Fig. 5) because only half the number of cells was present in the coinfection. If the titan cells produced by the wild-type strain protected the *gpr5Δ* cells from phagocytosis, then the amount of phagocytosis in the *gpr5Δ* strain should decrease in the coinfection.

Similar to experiments described above, phagocytosis of the *gpr5Δ* cells was significantly higher than phagocytosis of the wild-type cells in the individual infections (Fig. 5,  $P = 0.0003$ ). Upon coinfection, phagocytosis of the wild-type strain did not differ significantly from the hypothesized phagocytosis level based on the wild-type control infection ( $P = 0.071$ ). In contrast, the *gpr5Δ* strain exhibited significantly less phagocytosis than hypothesized based on the control *gpr5Δ* infection ( $P = 0.029$ ). Additionally, the total amount of phagocytosis in the coinfection was equivalent to that in the wild-type control infection and significantly less than that in the *gpr5Δ* control ( $P = 0.27$  and  $P = 0.0001$ , respectively). Taken together, these data show that the presence of titan cells produced by the wild-type strain was able to confer cross-protection to *gpr5Δ* cells during coinfection. These data support the hypothesis that titan cell production protects normal-size cryptococcal cells from phagocytosis.

**Size alone does not confer cross-protection from phagocytosis.** Macrophages can experience frustrated phagocytosis when a particle, such as a large asbestos particle, is too large to be engulfed (1). To determine whether the cross-protection of normal-size cells from phagocytosis could be due to the large size of the titan cells, mice were coinfectd with inert beads to mimic the differences in size observed during the cryptococcal infections. Large 30- $\mu$ m beads were used to simulate the titan cell size, while small 10- $\mu$ m beads were used to simulate normal-size cryptococcal cells. Beads were opsonized as described previously to stimulate phagocytosis, and an approximate 1:1 ratio of large and small beads was used to simulate maximal titan cell production during cryptococcal infections. In contrast to the cryptococcal infections, the presence of large beads did not provide protection from phagocytosis to the small beads (Fig. 1B). These data show that the presence of 30- $\mu$ m particles does not provide protection from phagocytosis to smaller particles and suggest that titan cells are providing cross-protection to normal-size cryptococcal cells through mechanisms other than cell size.

## DISCUSSION

Cryptococcal titan cells exhibit characteristics that may protect the cells from the host immune response. Titan cells are resistant to oxygen and nitrogen free radicals released by host immune cells to kill pathogens (15, 25). In addition, the highly cross-linked capsule and thickened cell wall of titan cells may act as defensive barriers, making it very difficult for host immune cells to gain access to the titan cell (25). Perhaps most intriguing is the obser-

vation that titan cells are not phagocytosed by cells of the host immune system and have altered antibody and complement binding (15, 25). We further explored the interaction between host phagocytes and cryptococcal cells during the pulmonary infection.

Titan cell production affects phagocytosis during cryptococcal infections in a nonlinear manner. As few as 5 to 10% titan cells in the entire cryptococcal cell population almost completely abolished phagocytosis of the cryptococcal cells. Less than 5% titan cell production resulted in significantly higher rates of phagocytosis, while titan cell production above 10% did not provide additional protection. While higher levels of titan cell production do not have deleterious effects on cryptococcal survival in the lungs, overproduction of titan cells in the lungs can inhibit cryptococcal dissemination to the central nervous system (15). This may explain why only a small proportion of the total population converts to titan cells during the infectious process.

Protection from phagocytosis was most apparent within the first 24 h postinfection. Typical human exposure to *C. neoformans* from the environment is likely to be a low number of desiccated yeast cells or spores. Titan cell production and subsequent protection from phagocytosis within the first 24 h may increase the population of the initial inoculum that can survive the early phagocytic immune response to establish the pulmonary infection.

Titan cells are typically 30  $\mu\text{m}$  or more in diameter, with some titan cells as large as 50 to 100  $\mu\text{m}$  in diameter (15, 25). Thus, titan cells are much larger than resident alveolar macrophages that are typically only 10 to 20  $\mu\text{m}$  in diameter (1). Using simulations with inert beads, we showed that the large size of titan cells can be protective against phagocytosis. Yet, titan cells also provide cross-protection to normal-size cells during early pulmonary infection. Previous studies have shown that large particles, such as asbestos particles, cannot be phagocytosed and induce a phenomenon referred to as “frustrated” phagocytosis (1, 22). Frustrated phagocytosis leads to reductions in overall phagocytosis and can lead to the production of interleukin-1 $\beta$  (IL-1 $\beta$ ), which induces a strong inflammatory response (10, 13, 14). We cannot rule out the possibility that titan cell formation may induce changes in the immune response that overlap frustrated phagocytosis. However, inoculation of mice with large inert beads of equivalent size to titan cells did not confer protection from phagocytosis to small beads equivalent in size to normal-size cryptococcal cells—even though host cells could not phagocytose the larger beads. These data suggest that other mechanisms beyond frustrated phagocytosis alone may be contributing to the protection of non-titan cells from phagocytosis. Instead, titan cell production may alter the host immune response by modulating immune activity through other mechanisms.

Titan cells could directly alter the activity of host phagocytes through cell-cell contact or close proximity. The capsule of *Haemophilus influenzae* has been shown to inhibit recognition and prevent uptake of cells that come in direct contact with macrophages (12). The M protein produced by *Streptococcus pyogenes* can inhibit engulfment by blocking complement binding to the bacterial cell surface and subsequent recognition by host macrophages (2, 23). Thus, the altered capsule produced by titan cells may be able to modulate the phagocytic activity of host cells through direct cell-cell contact.

It is also possible that titan cells could stimulate killing of phagocytes, either by toxin production or by morphological

switch. Exotoxin A produced by *Pseudomonas aeruginosa* is one of several bacterial toxins that have been shown to be cytotoxic to macrophages, inhibiting phagocytic activity and causing cell death (19). *C. neoformans* has been shown to produce extracellular vesicles that contain immune modulating compounds (17, 20). Titan cells have large vacuoles with abundant multivesicular bodies (25; J. Choi, A. W. Vogl, and J. W. Kronstad, submitted for publication), suggesting extracellular vesicle formation may be enhanced in titan cells. Titan cells could also produce modified vesicles containing compounds that could modulate the immune response or kill host cells.

Engulfment of a normal-size cryptococcal cell by resident alveolar macrophages could stimulate titan cell production. The rapid cell enlargement associated with titan cell formation could lyse the macrophage. The commensal fungus *Candida albicans* is stimulated to switch from the easily phagocytosed yeast form to the hyphal form upon phagocytosis. The hyphae eventually grow too large to be contained by the host cells and will ultimately lyse the macrophage and escape killing (5, 9).

Alternatively, titan cell production may alter the host immune response systemically rather than locally. Altered host-pathogen interactions, as exhibited in the presence of titan cells, may result in altered recruitment of host cells to the lungs. Reduced recruitment of phagocytes, such as monocytes, to the lungs could result in a lower phagocyte/cryptococcal cell ratio. The increase in phagocytosis observed in titan cell mutants such as the *gpr5 $\Delta$*  and *gpr4 $\Delta$  gpr5 $\Delta$*  strains may be the result of increased recruitment of host cells to the lungs compared to the wild-type infection. Microscopic examination of the titan-cell-deficient infections did reveal large aggregates of host cells that are lacking in the wild-type infection (Okagaki and Nielsen, unpublished), indicating that either recruitment or adhesion is altered in the presence of titan cells. *Streptococcus* species produce the small molecule streptolysin S, which inhibits chemotaxis and recruitment of neutrophils, reducing the inflammatory response at the site of infection (8). *Clostridium perfringens* produces a toxin similar in structure to streptolysin S, called  $\theta$  toxin, which also prevents chemotaxis of phagocytes (21). Thus, titan cells may be inhibiting phagocytosis by modulating the influx of leukocytes via the production of a small molecule chemotaxis inhibitor.

The data presented here are the first evidence that titan cell production in *C. neoformans* protects normal-size cells from phagocytosis in the host pulmonary environment. Therefore, titan cell production by *C. neoformans* may be instrumental in the initial establishment of infection, promoting increased fungal burden in the lungs. While the mechanism of this protection from phagocytosis remains unknown, studies from other organisms suggest that titan cell production likely results in a dramatic remodeling of the host pulmonary immune response. This remodeling could occur either through direct interactions or through production of small molecules, resulting in a reduction in global phagocytosis rates and subsequent promotion of cryptococcal survival within the host.

## ACKNOWLEDGMENTS

This work was supported by NIH grant AI080275 to K.N. L.H.O. was also supported by the Dennis W. Watson Fellowship and a Doctoral Dissertation Fellowship from the University of Minnesota.

## REFERENCES

1. Cannon GJ, Swanson JA. 1992. The macrophage capacity for phagocytosis. *J. Cell Sci.* 101:907–913.
2. Courtney HS, Hasty DL, Dale JB. 2006. Anti-phagocytic mechanisms of *Streptococcus pyogenes*: binding of fibrinogen to M-related protein. *Mol. Microbiol.* 59:936–947.
3. D'Souza CA, et al. 2001. Cyclic AMP-dependent protein kinase controls virulence of the fungal pathogen *Cryptococcus neoformans*. *Mol. Cell. Biol.* 21:3179–3191.
4. Fan W, Kraus PR, Boily MJ, Heitman J. 2005. *Cryptococcus neoformans* gene expression during murine macrophage infection. *Eukaryot. Cell* 4:1420–1433.
5. Ghosh S, et al. 2009. Arginine-induced germ tube formation in *Candida albicans* is essential for escape from murine macrophage line RAW 264.7. *Infect. Immun.* 77:1596–1605.
6. Heitman J. 2011. *Cryptococcus*: from human pathogen to model yeast. ASM Press, Washington, DC.
7. Hsueh YP, Xue C, Heitman J. 2007. G protein signaling governing cell fate decisions involves opposing G $\alpha$  subunits in *Cryptococcus neoformans*. *Mol. Biol. Cell* 18:3237–3249.
8. Lin A, Loughman JA, Zinselmeyer BH, Miller MJ, Caparon MG. 2009. Streptolysin S inhibits neutrophil recruitment during the early stages of *Streptococcus pyogenes* infection. *Infect. Immun.* 77:5190–5201.
9. Lorenz MC, Bender JA, Fink GR. 2004. Transcriptional response of *Candida albicans* upon internalization by macrophages. *Eukaryot. Cell* 3:1076–1087.
10. Netea MG, et al. 2010. IL-1 $\beta$  processing in host defense: beyond the inflammasomes. *PLoS Pathog.* 6:e1000661. doi:10.1371/journal.ppat.1000661.
11. Nielsen K, et al. 2003. Sexual cycle of *Cryptococcus neoformans* var. *grubii* and virulence of congenic  $\alpha$  and  $\alpha$  isolates. *Infect. Immun.* 71:4831–4841.
12. Noel GJ, Hoiseth SK, Edelson PJ. 1992. Type b capsule inhibits ingestion of *Haemophilus influenzae* by murine macrophages: studies with isogenic encapsulated and unencapsulated strains. *J. Infect. Dis.* 166:178–182.
13. Oghiso Y, Kubota Y. 1986. Enhanced interleukin 1 production by alveolar macrophages and increase in Ia-positive lung cells in silica-exposed rats. *Microbiol. Immunol.* 30:1189–1198.
14. Oghiso Y, Kubota Y. 1987. Interleukin 1 production and accessory cell function of rat alveolar macrophages exposed to mineral dust particles. *Microbiol. Immunol.* 31:275–287.
15. Okagaki LH, et al. 2010. Cryptococcal cell morphology affects host cell interactions and pathogenicity. *PLoS Pathog.* 6:e1000953. doi:10.1371/journal.ppat.1000953.
16. Okagaki LH, et al. 2011. Cryptococcal titan cell formation is regulated by G-protein signaling in response to multiple stimuli. *Eukaryot. Cell* 10:1306–1316.
17. Oliveira DL, et al. 2010. Extracellular vesicles from *Cryptococcus neoformans* modulate macrophage functions. *Infect. Immun.* 78:1601–1609.
18. Park BJ, et al. 2009. Estimation of the current global burden of cryptococcal meningitis among persons living with HIV/AIDS. *AIDS* 23:525–530.
19. Pollack M, Anderson SE, Jr. 1978. Toxicity of *Pseudomonas aeruginosa* exotoxin A for human macrophages. *Infect. Immun.* 19:1092–1096.
20. Rodrigues ML, et al. 2008. Extracellular vesicles produced by *Cryptococcus neoformans* contain protein components associated with virulence. *Eukaryot. Cell* 7:58–67.
21. Stevens DL, Mitten J, Henry C. 1987. Effects of  $\alpha$  and  $\theta$  toxins from *Clostridium perfringens* on human polymorphonuclear leukocytes. *J. Infect. Dis.* 156:324–333.
22. Takemura R, Stenberg PE, Bainton DF, Werb Z. 1986. Rapid redistribution of clathrin onto macrophage plasma membranes in response to Fc receptor-ligand interaction during frustrated phagocytosis. *J. Cell Biol.* 102:55–69.
23. Thern A, Wastfelt M, Lindahl G. 1998. Expression of two different antiphagocytic M proteins by *Streptococcus pyogenes* of the OF+ lineage. *J. Immunol.* 160:860–869.
24. Xue C, Bahn YS, Cox GM, Heitman J. 2006. G protein-coupled receptor Gpr4 senses amino acids and activates the cAMP-PKA pathway in *Cryptococcus neoformans*. *Mol. Biol. Cell* 17:667–679.
25. Zaragoza O, et al. 2010. Fungal cell gigantism during mammalian infection. *PLoS Pathog.* 6:e1000945. doi:10.1371/journal.ppat.1000945.